Monthly Notices of the ROYAL ASTRONOMICAL SOCIETY

MNRAS **538,** 76–91 (2025) https://doi.org/10.1093/mnras/staf292
Advance Access publication 2025 February 17

The distribution of galaxy rotation in *JWST* Advanced Deep Extragalactic Survey

Lior Shamir ★
Kansas State University, Department of Computer Science, Manhattan, KS 66506, USA

Accepted 2025 February 12. Received 2025 February 12; in original form 2024 December 23

ABSTRACT

JWST provides a view of the Universe never seen before, and specifically fine details of galaxies in deep space. *JWST* Advanced Deep Extragalactic Survey (JADES) is a deep field survey, providing unprecedentedly detailed view of galaxies in the early Universe. The field is also in relatively close proximity to the Galactic pole. Analysis of spiral galaxies by their direction of rotation in JADES shows that the number of galaxies in that field that rotate in the opposite direction relative to the Milky Way galaxy is ∼50 per cent higher than the number of galaxies that rotate in the same direction relative to the Milky Way. The analysis is done using a computer-aided quantitative method, but the difference is so extreme that it can be noticed and inspected even by the unaided human eye. These observations are in excellent agreement with deep fields taken at around the same footprint by *Hubble Space Telescope* and *JWST*. The reason for the difference may be related to the structure of the early Universe, but it can also be related to the physics of galaxy rotation and the internal structure of galaxies. In that case the observation can provide possible explanations to other puzzling anomalies such as the H_o tension and the observation of massive mature galaxies at very high redshifts.

Key words: galaxies: general – galaxies: spiral – early Universe – large-scale structure of Universe.

1 INTRODUCTION

JWST has introduced unprecedented imaging power, allowing it to capture high visual details of astronomical objects in deep space. The ability to identify shapes of objects in the very early Universe has a transformative impact on astronomy and cosmology. An example is the galaxies identified at very high redshifts (Adams et al. 2023; Boylan-Kolchin 2023; Bradley et al. 2023; Carniani et al. 2024), such as JADES-GS-z14-0 at redshift of ∼14.2, and just ∼0.25 Gyr after the big bang (Carniani et al. 2024; Helton et al. 2024; Jones et al. 2025; Schouws et al. 2024). Galaxies at unexpectedly high redshift also include Milky Way-like spiral galaxies (Costantin et al. 2023; Jain & Wadadekar 2024), showing that such galaxies are also present at relatively high-redshift ranges (Kuhn et al. 2024). Although spiral galaxies at unexpectedly high redshifts were known before *JWST* was launched (Tsukui & Iguchi 2021), the visual observations enabled by *JWST* are considered surprising given the current cosmological and galaxy formation theories (Adil et al. 2023; Boylan-Kolchin 2023; Forconi et al. 2023; Gupta 2023; Melia 2023; Xiao et al. 2024).

Additionally, the yet unexplained H_o tension (Wu & Huterer 2017; Bolejko 2018; Mörtsell & Dhawan 2018; Davis et al. 2019; Camarena & Marra 2020; Pandey, Raveri & Jain 2020; Di Valentino et al. 2021; Riess et al. 2022) introduces a substantial challenge to cosmology, and it has been suggested that the H_o tension and high-redshift galaxies observed by *JWST* are linked (Shen et al. 2024). While research is bound to continue, the unexpected observations made so far by *JWST* have been argued to be in tension with standard cosmology (Dolgov 2023; Forconi et al. 2023; Gupta 2023, 2024a, b; Lovell et al. 2023; Wang & Liu 2023; Muñoz et al. 2024).

One of the observations enabled by the ability of *JWST* to identify high visual details of galaxies is the alignment between the galaxy direction of rotation as observed by *JWST* and the direction of rotation of the Milky Way (Shamir 2024e). Namely, *JWST* shows a much higher number of galaxies that rotate in the opposite direction relative to the Milky Way. That can be observed in *JWST* deep fields taken at close proximity to the Galactic pole. When spiral galaxies are located at around the Galactic pole, their direction of rotation can determine whether they rotate in the same direction relative to the Milky Way, or in the opposite direction relative to the Milky Way (Shamir 2024e).

A first observation of the higher prevalence of galaxies that rotate in opposite direction relative to the Milky Way in *JWST* deep fields was reported in Shamir (2024e). The analysis was based on a preliminary *JWST* deep field image taken inside the field of the *Hubble Space Telescope* (*HST*) Ultra Deep Field (UDF). The deep field was imaged in 2022 October, and the image was released to the public on 2023 April. Analysis of the field (Shamir 2024e) identified 33 galaxies with identifiable direction of rotation, where 23 of them rotated in the opposite direction relative to the Milky Way ($p \simeq 0.012$). Fig. 1 shows the deep field annotated by the direction of rotation of the galaxies (Shamir 2024e).

When done manually, the determination of the direction of rotation of a galaxy can be a subjective task, as different annotators might have different opinions regarding the direction towards a galaxy

★ E-mail: lshamir@mtu.edu

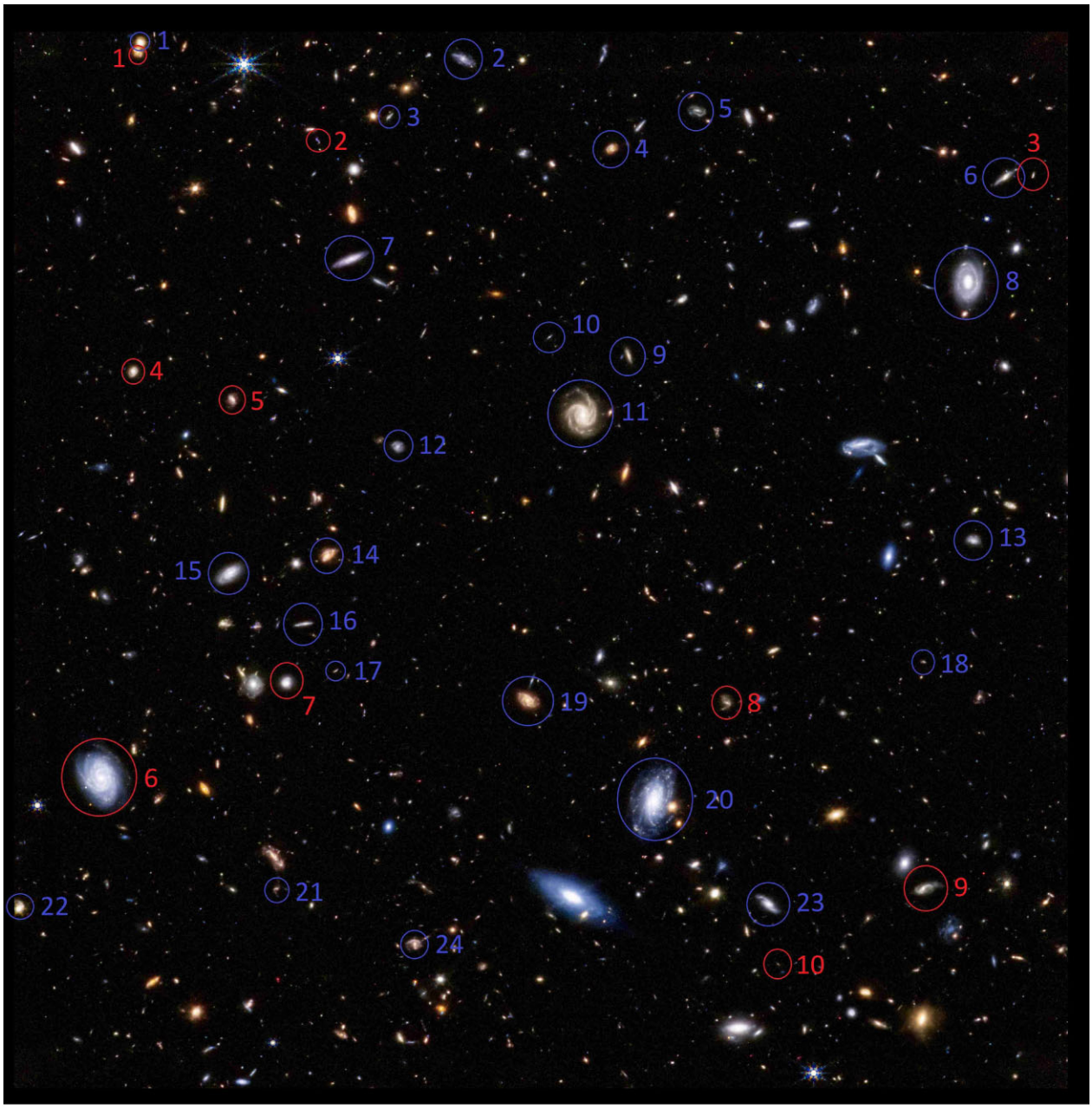

Figure 1. Spiral galaxies imaged by *JWST* that rotate in the same direction relative to the Milky Way (red) and in the opposite direction relative to the Milky Way (blue). The number of galaxies rotating in the opposite direction relative to the Milky Way as observed from Earth is far higher (Shamir 2024e).

rotates. A simple example is the crowdsourcing annotation through Galaxy Zoo 1 (Land et al. 2008), where in the vast majority of the galaxies different annotators provided conflicting annotations. Therefore, the annotations shown in Fig. 1 were made by a computer analysis that followed a defined symmetric model (Shamir 2024e). Yet, the advantage of the analysis of the relatively small *JWST* deep field is that it can be inspected by the human eye to ensure that the annotations of the galaxies are consistent, and that no population of non-annotated galaxies that could change the outcome of the analysis exists (Shamir 2024e).

The difference between the number of galaxies that rotate in opposite directions was also noticed when using Earth-based telescopes (MacGillivray & Dodd 1985; Longo 2011; Shamir 2012, 2016, 2019, 2020b, c, d, 2021a, b, 2022a, b, d, e). Namely, it has been shown that the difference between the number of galaxies that rotate in opposite direction increases as the redshift gets higher (Shamir 2019, 2020d, 2022d, 2024d), which might suggest that the difference becomes larger in the deep Universe as imaged by *JWST*. On the other hand, several studies argued that the distribution is random (Iye & Sugai 1991; Land et al. 2008; Hayes, Davis & Silva 2017; Tadaki et al. 2020; Iye, Yagi & Fukumoto 2021; Patel & Desmond 2024). These studies will be discussed in Section 4 of this paper. But with the imaging power of *JWST*, the uneven distribution becomes clear, and can be verified even with the unaided human eye (Shamir 2024e). This paper analyses the distribution of spiral galaxies in the JADES survey. Any anomaly in the distribution can be related to the structure of the early universe, but can also be driven by the mysterious physics of galaxy rotation.

While several analyses using different instruments were performed, *JWST* introduces new opportunities to study the asymmetry in the early Universe. The imaging power of *JWST* is particularly meaningful because the magnitude of the asymmetry has been identified to grow as the redshift gets larger (Shamir 2019, 2020d, 2022d, 2024d), and therefore studying the asymmetry in deep fields can lead to new observations. This paper examines the possibility of an anomaly in the distribution of galaxies rotating in opposite directions in the *JWST* deep fields as observed from Earth. The observation is compared to analyses with other space- and Earth-based telescopes that image the same field, as well as other parts of the entire sky.

2 DATA

The data used in this analysis is taken from the GOODS-S field of *JWST* Advanced Deep Extragalactic Survey (JADES). JADES (Eisenstein et al. 2023; Bunker et al. 2024) is the largest deep field imaging program planned for the early operation of *JWST*, focusing on the well-studied Great Observatories Origins Deep Survey South (GOODS-S) and Great Observatories Origins Deep Survey North (GOODS-N) fields. The image data are acquired primarily through the near-infrared camera (NIRCam).

The image data used for the analysis was based on the *JWST* 4.4, 2.0, and 0.9 μm bands visualized through the red giant branch channels, providing and informative form of visualization that allows for effective analysis. Parts of the JADES GOODS-S field that did not have these three channels were not used in the analysis. The RA of the objects used in this study ranged from 53.01885° to 53.2184°, and the declination ranged between −27.9145° to −27.7292°.

The galaxies were annotated by their direction of rotation as done in Shamir (2024e). The analysis was automatic, and followed a defined model that allows to define the direction of rotation of a galaxy in an objective and consistent manner. As also briefly mentioned in Introduction, manual annotation of the direction of rotation of a galaxy can be subjective, and different people might have different opinions when they need to determine the direction of rotation of a galaxy. It has also been shown that such annotation can be driven by consistent biases, so even a group of people annotating the same galaxy cannot provide consistent annotations in all cases (Land et al. 2008). For that reason, while manual annotation should be used to verify the consistency of the annotation, it cannot be considered a sound scientific methodology that such annotation can rely on.

Deep convolutional neural networks (CNNs) have become the most common solution to tasks related to image classification tasks. Their popularity is driven by excellent performance, as well as the availability of easy-to-use libraries that make the analysis accessible also to researchers who do not necessarily have strong computing skills. The primary downside of CNNs is that they are driven by highly complex data-driven rules that are very difficult to understand. Therefore, they are subjected to biases that can be highly difficult to identify (Dhar & Shamir 2021; Ball 2023; Erukude, Joshi & Shamir 2024). Such biases can be driven by the manual selection of training samples, as two neural networks trained with two different training sets will also perform differently. In the case of astronomical images, even the distribution of the training galaxy images in the sky can lead to different results (Dhar & Shamir 2022). Therefore, using CNNs for the annotation of the galaxies cannot be considered a sound solution when the analysis needs to be clear, and certain conditions such as the symmetry of the algorithm need to be guaranteed.

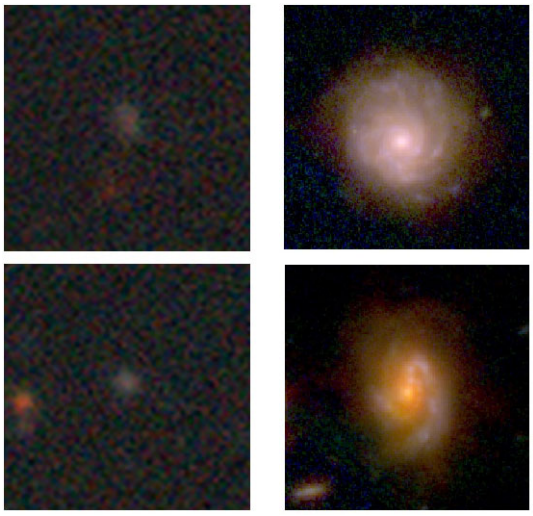

Figure 2. Example of the same galaxies imaged by DES (left) and by *JWST*. *JWST* allows to analyse galaxies that DES or other Earth-based telescopes cannot image with sufficient details to identify their direction of rotation.

Clearly, the annotation of the galaxies is not complete, as some of the galaxies are not assigned with a direction of rotation, and are therefore excluded from the analysis. Some of the galaxies may be elliptical, and other galaxies may not have clear visual details that are sufficient to identify their direction of rotation. Fig. 2 shows examples of galaxies imaged by both Dark Energy Survey (DES) and *JWST*. While the DES images do not provide sufficient visual details, the *JWST* images allow to identify the direction of rotation of the galaxies. Therefore, *JWST* can provide an analysis of the direction of rotation of galaxies that cannot be imaged by DES or by any other existing Earth-based telescope.

The annotations were done by using the Ganalyzer algorithm (Shamir 2011a, b) and also used in Shamir (2011b, 2013, 2016, 2017a, b, c, 2020b, c, 2021a, b, 2022b, d, e, 2024e). The algorithm is based on a first step of separating foreground objects from the background. After each object is separated from the image, it is transformed into its radial intensity plot transformation.

The radial intensity plot captures the object intensity variations at different distances from its centre. It is a 35 × 360 matrix, where the intensity of the pixel (x, y) is the median intensity of the 5 × 5 pixels centred at $(O_x + \sin(\theta) \cdot r, O_y - \cos(\theta) \cdot r)$ in the original image, where r is the radial distance from the centre (O_x, O_y), and θ is the polar angle (Shamir 2011b).

Because the arms of a galaxy are brighter than the non-arm part of the galaxy at the same distance from the galaxy centre, the arm pixels can be identified by a peak detection algorithm (Morháč et al. 2000) applied to each line in the radial intensity plot. Applying a linear regression to the peaks provides the slope of the line formed by them, and the sign of the slope determines the direction towards which the arm of the galaxy is curved. To avoid elliptical galaxies or galaxies that do not have a clear direction of rotation, galaxies that have less than 30 peaks are considered galaxies that do not have an identifiable direction of rotation. Also, the slope of the linear regression needs to be at least 0.35 (Shamir 2011b), otherwise the galaxy is not assigned with a direction of rotation, and therefore is not used in the analysis. Fig. 3 shows examples of galaxies as imaged by *JWST* as used in this study, and their radial intensity plots that allow to identify their direction of rotation. The process is described with empirical analysis and experimental results in Shamir (2011b,

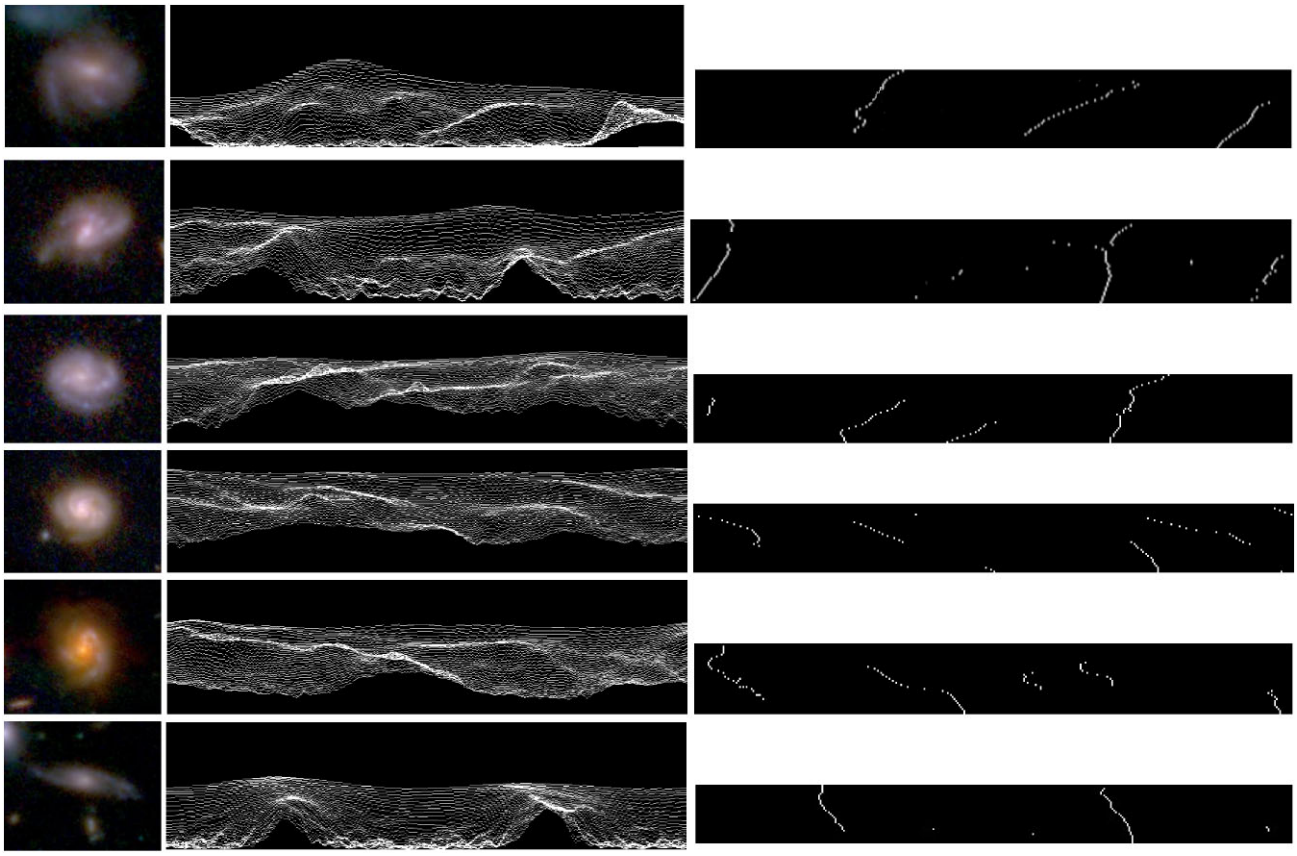

Figure 3. Example of galaxies imaged by *JWST* and the peaks of the radial intensity plot transformations of each image. The lines formed by the peaks allow to identify the direction of the curve of the arms, and consequently the spin direction of the galaxy.

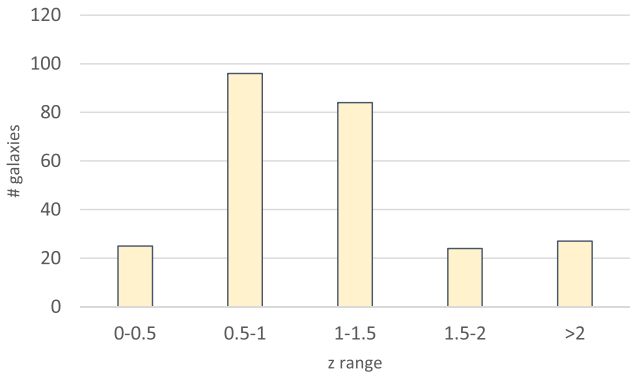

Figure 4. The redshift distribution of the *JWST* galaxies used in the study.

2013, 2016, 2017a, b, c, 2020b, c, 2021a, b, 2022b, d, e). Namely, it has been used to analyse initial *JWST* deep field images taken inside the footprint of GOODS-S (Shamir 2024e).

The process led to 263 galaxies with identified direction of rotation. Fig. 4 shows the distribution of the redshift of the galaxies.

While the algorithm is defined and symmetric, to ensure the symmetric nature of the analysis the entire field was mirrored, and the algorithm was applied to the mirrored image. Results were exactly inverse, which can be expected since the algorithm is symmetric, and was tested in a similar manner in previous experiments (Shamir 2011b, 2013, 2016, 2017a, b, c, 2020b, c, 2021a, b, 2022b, d, e, 2024e).

The annotation algorithm determines the directions of rotation of the galaxies by the curves of the arms. The arms of spiral galaxies have been shown to be a very reliable probe for determining the direction of rotation of the stellar mass as it rotates around the galaxy centre. For instance, De Vaucouleurs (1958) used the galaxy spectra and dust silhouette to study the link between the direction of rotation and shape of the galaxy arms, and found that in all cases the spiral arms were trailing. A more recent study (Iye, Tadaki & Fukumoto 2019) also found that all galaxies that were examined have trailing arms, and therefore the shape of the arm is a strong indication of the direction of rotation of the stellar mass. In some very rare cases galaxies can also have leading arms. A known example of a galaxy with leading arms is NGC 4622 (Freeman, Byrd & Howard 1991; Byrd & Howard 2019), but these cases are extremely rare.

3 RESULTS

The application of the image processing to the *JWST* GOODS-S image data as described in Section 2 provided annotations for 263 galaxies that their direction of rotation was identified. Of these galaxies, 105 rotate counterclockwise, while 158 rotate clockwise. Assuming that the probability of a galaxy to rotate in a certain direction is completely random, the one-tailed binomial distribution probability to have such asymmetry or stronger by chance is $\sim$0.0007, which is $\sim 3.39\sigma$.

Figs 5 and 6 show the galaxies in the field that were identified as rotating in the same direction relative to the Milky Way (counterclockwise) and the galaxies that rotate in the opposite direction

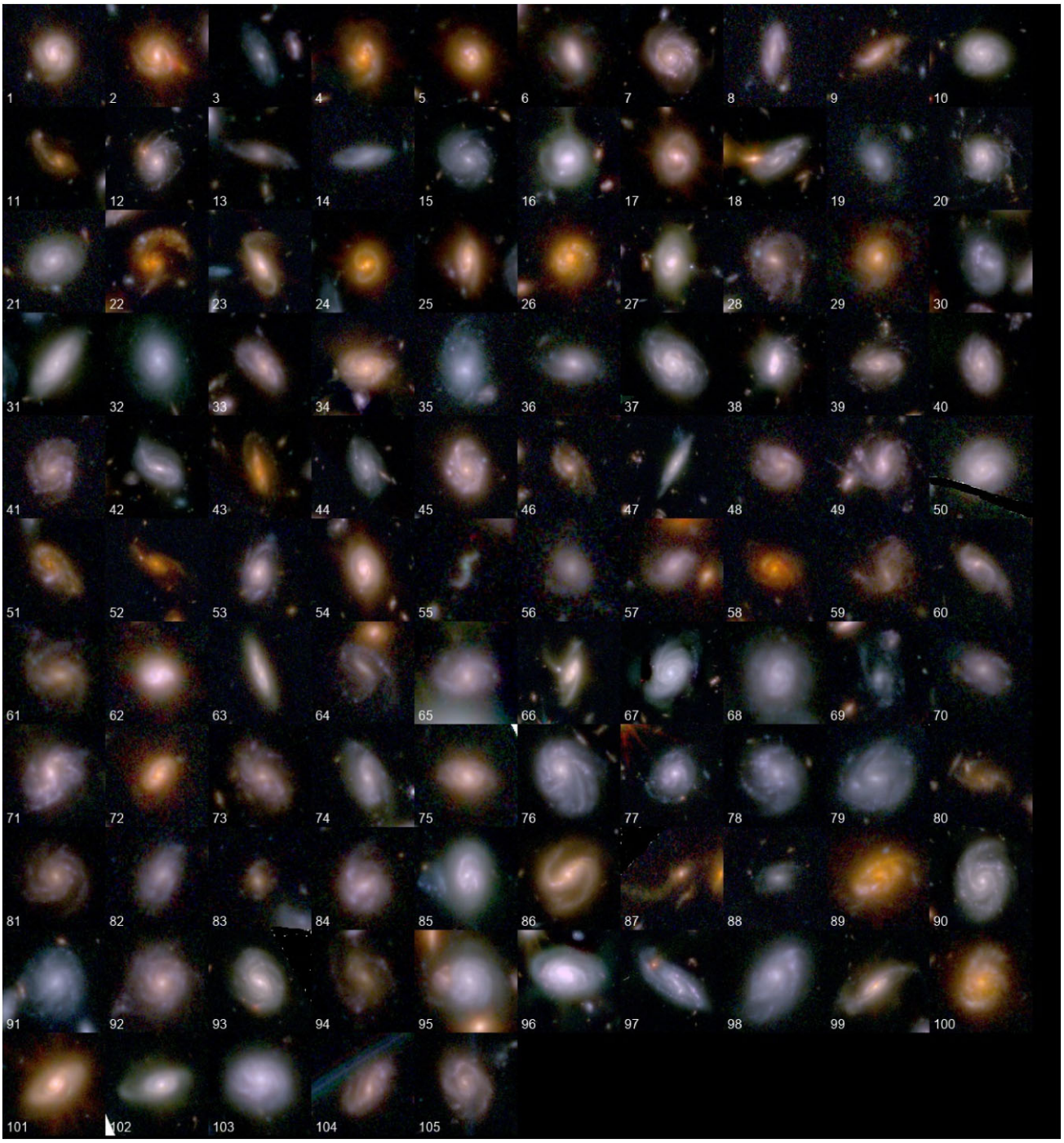

Figure 5. The galaxies in the JADES GOODS-S field that were identified as rotating in the same direction relative to the Milky Way (counterclockwise). The (α, δ) coordinates of each galaxy are specified in Table 1.

relative to the Milky Way (clockwise), respectively. Tables 1 and 2 provide the coordinates of each of the 263 galaxies. Fig. 7 shows the location of the galaxies inside the JADES GOODS-S field. While the unaided human eye might not be a fully sound tool to annotate the galaxies, visual inspection shows consistency between the annotation of the algorithm and the human eye, and no galaxy seems to be identified incorrectly.

Visual inspection of the galaxies that were identified shows no galaxy that was annotated incorrectly. But the annotation algorithm also avoids annotating galaxies that their direction of rotation cannot be identified. These may be elliptical galaxies, or galaxies that the visual details of their arms do not allow the identification of their direction of rotation. Because the algorithm is symmetric, galaxies that their direction of rotation could not be identified by the algorithm are expected to be treated in the same manner regardless of their direction of rotation. Still, it is important to also inspect the population of galaxies that the algorithm could not identify their direction of rotation.

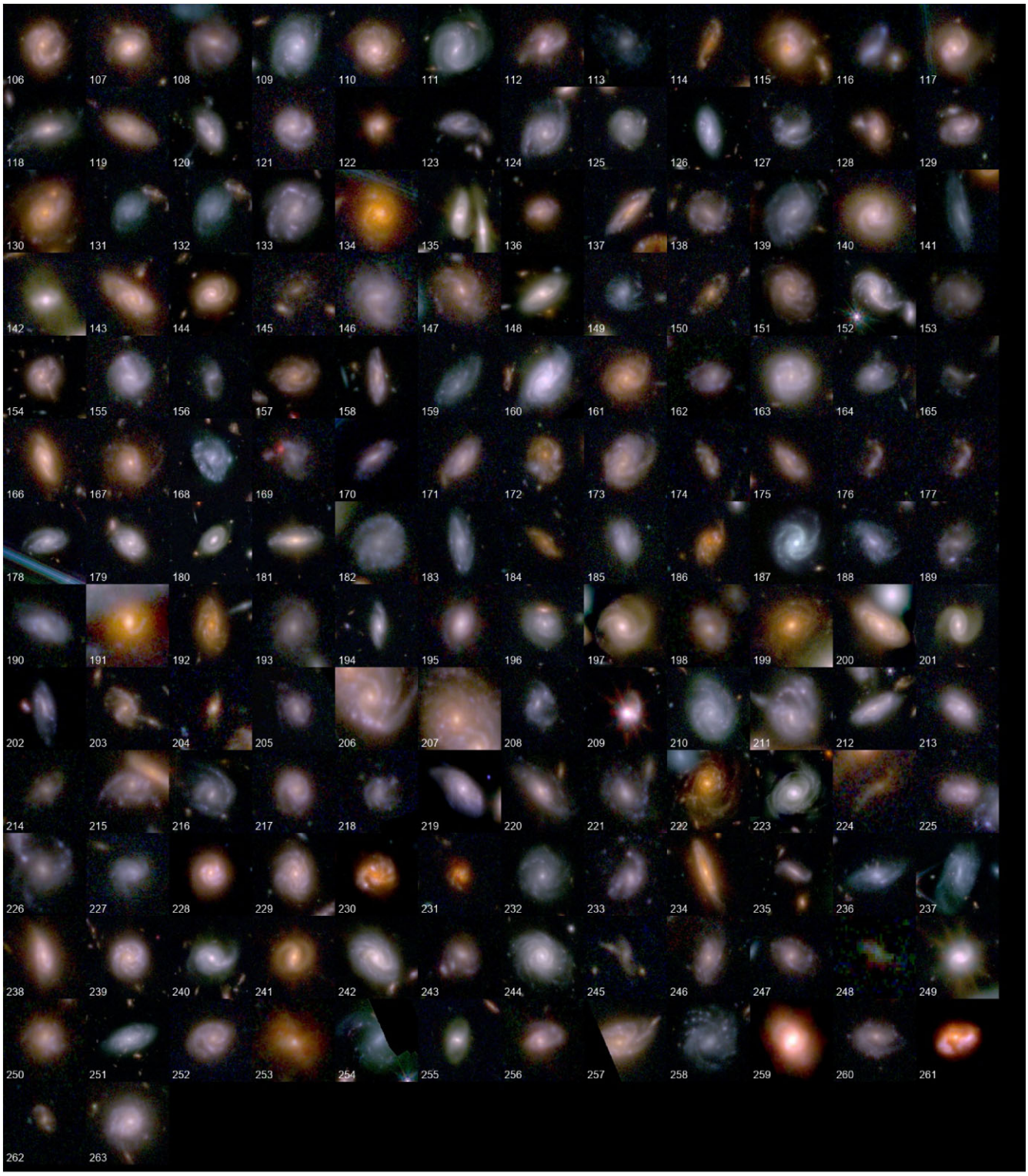

Figure 6. The galaxies in the JADES GOODS-S field that were identified as rotating in the opposite direction relative to the Milky Way. The coordinates of each galaxy are specified in Table 2.

As was done in Shamir (2024e), the field was inspected manually to identify galaxies that their direction of rotation was not identified by the algorithm. Figs 8 and 9 show galaxies that perhaps could be considered as rotating counterclockwise and clockwise, respectively. The rotation of direction is not entirely clear in these images, but these galaxies were the most clear galaxies among those galaxies that were not identified by the algorithm. As mentioned before, manual observation is not a sound scientific manner to identify the

Table 1. The RA and Dec. of the galaxies that rotate counterclockwise shown in Fig. 5.

Numbers	RA	Dec.	Numbers	RA	Dec.	Numbers	RA	Dec.
1	53.0287575	−27.8703469	2	53.0305730	−27.8557305	3	53.0346279	−27.8713092
4	53.0367451	−27.8875751	5	53.0373338	−27.8703302	6	53.0425003	−27.8821344
7	53.0442441	−27.8953532	8	53.0460538	−27.8289356	9	53.0467626	−27.8520855
10	53.0495568	−27.8992607	11	53.0508248	−27.8919429	12	53.0514024	−27.8701501
13	53.0552519	−27.8856482	14	53.0558147	−27.8300434	15	53.0567343	−27.8796932
16	53.0578412	−27.8307351	17	53.0585653	−27.8568762	18	53.0605633	−27.8512857
19	53.0606090	−27.8310224	20	53.0625037	−27.8349052	21	53.0629972	−27.8310975
22	53.0689231	−27.8796888	23	53.0704161	−27.9052013	24	53.0717760	−27.8437142
25	53.0720162	−27.8537413	26	53.0727344	−27.8343114	27	53.0752012	−27.8314599
28	53.0772016	−27.8205387	29	53.0778957	−27.8932042	30	53.0781977	−27.8701926
31	53.0782543	−27.8569828	32	53.0794105	−27.8623380	33	53.0796836	−27.8424121
34	53.0803383	−27.9005456	35	53.0803688	−27.8083994	36	53.0810023	−27.8238445
37	53.0819773	−27.8399439	38	53.0844410	−27.8728831	39	53.0878515	−27.8308227
40	53.0951927	−27.8568509	41	53.0956144	−27.8159647	42	53.1018111	−27.8650500
43	53.1031616	−27.8652455	44	53.1074863	−27.8623169	45	53.1077205	−27.8388817
46	53.1081399	−27.8877607	47	53.1083292	−27.8795013	48	53.1085802	−27.8633293
49	53.1103699	−27.8883061	50	53.1107677	−27.8339117	51	53.1108220	−27.8006488
52	53.1131144	−27.8866044	53	53.1155528	−27.9144036	54	53.1155789	−27.8447307
55	53.1187014	−27.8057706	56	53.1237878	−27.8326410	57	53.1239903	−27.8631171
58	53.1245910	−27.8932989	59	53.1262410	−27.8292075	60	53.1272777	−27.8386627
61	53.1301701	−27.7809458	62	53.1326939	−27.8329912	63	53.1338997	−27.8516127
64	53.1352184	−27.8750690	65	53.1373614	−27.7622325	66	53.1374871	−27.8418249
67	53.1437771	−27.8134799	68	53.1454738	−27.7506179	69	53.1454750	−27.8336683
70	53.1462674	−27.8314869	71	53.1499913	−27.7399957	72	53.1507510	−27.8574200
73	53.1508711	−27.7419219	74	53.1523853	−27.8343908	75	53.1554348	−27.7661381
76	53.1564312	−27.8108991	77	53.1564439	−27.8710278	78	53.1581806	−27.7811417
79	53.1589977	−27.8326493	80	53.1595345	−27.8392275	81	53.1598219	−27.7623367
82	53.1600056	−27.7669025	83	53.1603471	−27.8406146	84	53.1618000	−27.7292176
85	53.1624406	−27.7751180	86	53.1635603	−27.7589436	87	53.1637381	−27.8514252
88	53.1643375	−27.8658913	89	53.1675906	−27.8304041	90	53.1698898	−27.7710453
91	53.1726089	−27.7964452	92	53.1754466	−27.7496166	93	53.1801809	−27.7989112
94	53.1852851	−27.7685314	95	53.1862976	−27.8230718	96	53.1868309	−27.7910178
97	53.1879238	−27.7940122	98	53.1902891	−27.7401635	99	53.1951860	−27.7538285
100	53.2015172	−27.7472044	101	53.2023884	−27.7513782	102	53.2046668	−27.7553699
103	53.2064105	−27.7750928	104	53.2131711	−27.7718123	105	53.2181259	−27.7658299

direction of rotation of the galaxies due to its subjective nature. These galaxies were not used in the analysis, but just to inspect the kind of galaxies that were not annotated by the algorithm. The manual inspection does not show a certain pattern of galaxies that their direction of rotation was not identified by the algorithm. The coordinates of the galaxies in both figures are specified in Tables 3 and 4.

JWST provides visual details of galaxies in the deep Universe, and far deeper than any other telescope. But the unequal number of galaxies that rotate in opposite directions around the Galactic poles was noticed also with Earth-based telescopes, although the differences were smaller than the difference observed in the deeper Universe using *JWST*. For instance, Fig. 10 shows the difference between the number of galaxies with opposite directions of rotation in different parts of the sky, as determined by using a large dataset of 1.3×10^6 galaxies annotated by their direction of rotation (Shamir 2022e). The galaxy images were collected by the Dark Energy Spectroscopic Instrument (DESI) Legacy Survey, and the analysis was done before *JWST* was launched. The difference between galaxies that rotate in opposite directions in the different parts of the sky are quantified by $\frac{cw-ccw}{cw+ccw}$ in the hemisphere centred at each integer (α, δ) combination, and displayed by the colour such that red parts of the sky indicate a higher number of galaxies rotating clockwise, and blue parts of the sky reflect a higher number of galaxies rotating counterclockwise. The figure shows simple direct measurements of the differences in different parts of the sky, and not an attempt to fit the distribution to a certain pre-determined model. The image and the analysis through which it was generated are explained in full detail in Shamir (2022e).

The figure shows a higher asymmetry in both ends of the Galactic poles, where in both end there is a higher number of galaxies that rotate in the opposite directions relative to the Milky Way galaxy. GOODS-S is located in relatively close proximity to the Southern Galactic pole, and therefore the difference can be expected based on previous observations made before *JWST* was launched. Previous observations using Earth-based telescopes also showed that the magnitude of the asymmetry increases as the redshift gets higher (Shamir 2020d). If that trend continues into the higher redshift ranges, it can also explain the higher asymmetry in the much higher redshift of the galaxies imaged by *JWST*.

'Webb's First Deep Field' was also tested in the same manner, providing no statistically significant asymmetry with 21 galaxies rotating counterclockwise, and 19 galaxies that rotate clockwise (Shamir 2024e). That field is not close to neither ends of the Galactic pole, so asymmetry is not expected in that field based on the analysis done with DESI Legacy Survey (Shamir 2022e) before *JWST* was launched.

Table 2. The RA and Dec. of the galaxies that rotate clockwise shown in Fig. 6.

Numbers	RA	Dec.	Numbers	RA	Dec.	Numbers	RA	Dec.
106	3.1279542	−27.7715134	107	53.0193353	−27.8602004	108	53.0248564	−27.8832216
109	53.0281374	−27.8675260	110	53.0286673	−27.8737467	111	53.0289134	−27.8803077
112	53.0315505	−27.8515717	113	53.0357380	−27.8716810	114	53.0368943	−27.8572009
115	53.0373588	−27.8758075	116	53.0408007	−27.8817782	117	53.0446664	−27.8936859
118	53.0450450	−27.8818705	119	53.0465296	−27.8821387	120	53.0492605	−27.8700264
121	53.0499228	−27.8428186	122	53.0521408	−27.8920364	123	53.0533498	−27.8897312
124	53.0561208	−27.8427935	125	53.0569792	−27.8262655	126	53.0573808	−27.8919577
127	53.0595572	−27.8224721	128	53.0604167	−27.8924328	129	53.0620101	−27.8768390
130	53.0627890	−27.8489887	131	53.0638817	−27.8243501	132	53.0639208	−27.8243688
133	53.0642316	−27.8572046	134	53.0650035	−27.8981819	135	53.0673265	−27.8282897
136	53.0678622	−27.8592175	137	53.0693205	−27.8788218	138	53.0697243	−27.8758420
139	53.0710796	−27.8537283	140	53.0717995	−27.9025473	141	53.0722817	−27.8443486
142	53.0727420	−27.8012799	143	53.0731238	−27.9018674	144	53.0734710	−27.8746265
145	53.0745397	−27.7985159	146	53.0753324	−27.9002020	147	53.0772981	−27.8095869
148	53.0779581	−27.8582796	149	53.0780646	−27.7948371	150	53.0782010	−27.8081526
151	53.0832777	−27.8480718	152	53.0862719	−27.8617956	153	53.0864800	−27.8698430
154	53.0888870	−27.8681537	155	53.0893112	−27.8172391	156	53.0893392	−27.8302602
157	53.0897244	−27.8446916	158	53.0902375	−27.8479062	159	53.0917752	−27.8850705
160	53.0917947	−27.9079949	161	53.0921738	−27.8791953	162	53.0937000	−27.8554013
163	53.0942337	−27.8755992	164	53.0951142	−27.8262703	165	53.0951248	−27.8313279
166	53.0966713	−27.8793750	167	53.0970239	−27.8816290	168	53.0971496	−27.8146692
169	53.0973401	−27.9013593	170	53.0985649	−27.8976944	171	53.0998786	−27.8798943
172	53.1007743	−27.8312572	173	53.1025891	−27.8815702	174	53.1027136	−27.8357093
175	53.1039113	−27.8390226	176	53.1058087	−27.8334029	177	53.1058206	−27.8334083
178	53.1058432	−27.8984435	179	53.1060740	−27.8652313	180	53.1073507	−27.8267313
181	53.1091200	−27.8530365	182	53.1109910	−27.9067594	183	53.1125336	−27.8080579
184	53.1137720	−27.8435787	185	53.1152094	−27.8325756	186	53.1160406	−27.9121885
187	53.1207774	−27.8189708	188	53.1221556	−27.8654683	189	53.1242332	−27.8897040
190	53.1293315	−27.7709544	191	53.1308698	−27.8299421	192	53.1310120	−27.8236125
193	53.1315421	−27.7864976	194	53.1316813	−27.8345866	195	53.1356372	−27.7666907
196	53.1357641	−27.8484238	197	53.1362945	−27.7632657	198	53.1369272	−27.7907591
199	53.1370804	−27.8501197	200	53.1376604	−27.7632512	201	53.1378387	−27.8566923
202	53.1392775	−27.7807792	203	53.1413527	−27.8257550	204	53.1418679	−27.8253231
205	53.1470842	−27.7785246	206	53.1479323	−27.7740950	207	53.1481753	−27.7738463
208	53.1492580	−27.7636845	209	53.1499215	−27.8140455	210	53.1515470	−27.8549017
211	53.1519920	−27.7747388	212	53.1520962	−27.8351648	213	53.1531176	−27.8686182
214	53.1554066	−27.7382866	215	53.1572340	−27.7379451	216	53.1578600	−27.7975775
217	53.1580437	−27.8384650	218	53.1602537	−27.7693798	219	53.1607121	−27.7753929
220	53.1608299	−27.7500577	221	53.1608511	−27.7428529	222	53.1627502	−27.7391179
223	53.1631045	−27.8123967	224	53.1636135	−27.8516310	225	53.1646982	−27.8533656
226	53.1648402	−27.7560441	227	53.1657665	−27.8562203	228	53.1658978	−27.7816064
229	53.1661972	−27.7875825	230	53.1697386	−27.8239961	231	53.1719913	−27.8395618
232	53.1721962	−27.7651716	233	53.1729385	−27.7779153	234	53.1729692	−27.7446003
235	53.1740883	−27.7881150	236	53.1747265	−27.8408071	237	53.1747682	−27.7992826
238	53.1753216	−27.7393471	239	53.1762360	−27.7962420	240	53.1763802	−27.8306977
241	53.1765762	−27.7855088	242	53.1784236	−27.7683139	243	53.1796778	−27.7688462
244	53.1801045	−27.7492538	245	53.1808938	−27.7549298	246	53.1821319	−27.7358393
247	53.1835660	−27.7568481	248	53.1845989	−27.7447883	249	53.1879459	−27.7900924
250	53.1885059	−27.7452762	251	53.1901361	−27.7652570	252	53.1920889	−27.7872543
253	53.1922054	−27.7410196	254	53.2018256	−27.7642261	255	53.2018992	−27.7888604
256	53.2028329	−27.7650603	257	53.2047339	−27.7568440	258	53.2069528	−27.7849266
259	53.2070046	−27.7529810	260	53.2118685	−27.7544650	261	53.2146651	−27.7526799
262	53.2157378	−27.7691409	263	53.2180201	−27.7540485			

4 SUMMARY OF EXPERIMENTS SUGGESTING THAT THE DISTRIBUTION OF THE GALAXY DIRECTIONS OF ROTATION IS RANDOM

Section 1 mentions multiple studies using several different space- and Earth-based telescopes showing unequal distribution of the directions of rotation of galaxies (MacGillivray & Dodd 1985; Longo 2011; Shamir 2012, 2016, 2019, 2020b, c, d, 2021a, b, 2022a, b, d, e). Reports started as early as the 1980s (MacGillivray & Dodd 1985), and include Earth-based telescopes such as Sloan Digital Sky Survey (SDSS) (Shamir 2019, 2020d, 2021a, 2022d), the Panoramic Survey Telescope and Rapid Response System (Pan-STARRS) (Shamir 2020d), the DES (Shamir 2022a), and DESI Legacy Survey (Shamir 2021b, 2022e), as well as space-based telescopes such as *HST* (Shamir 2020b) and *JWST* (Shamir 2024e).

Section 1 also mentions previous reports suggesting fully random distribution of the directions of rotations of galaxies. Although none

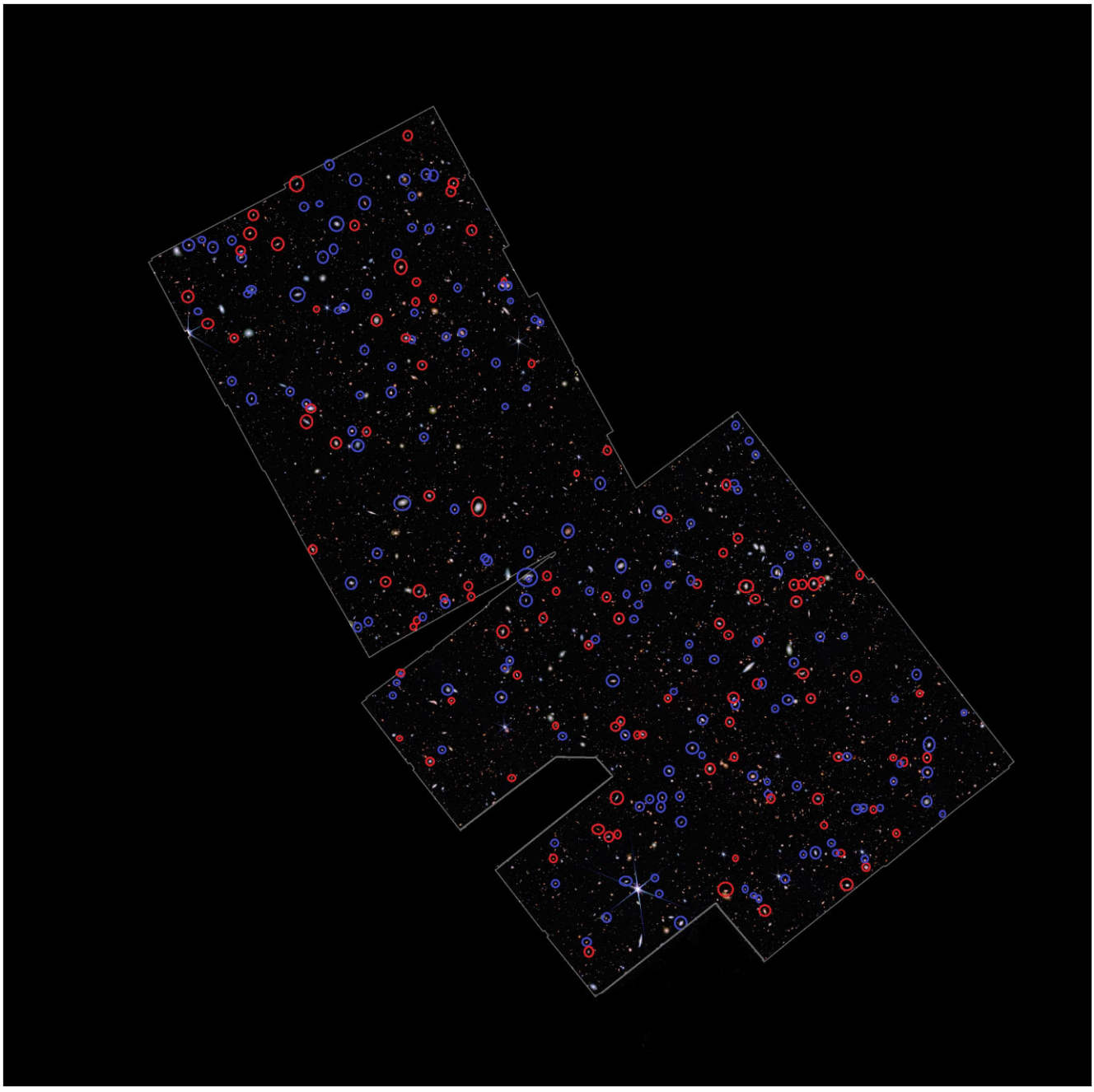

Figure 7. Spiral galaxies imaged by *JWST* in the GOODS-S field of JADES that rotate in the same direction relative to the Milky Way (red), and in the opposite direction relative to the Milky Way (blue). The figure shows 158 galaxies that rotate in the opposite direction relative to the Milky Way, and just 105 that rotate in the same direction relative to the Milky Way. The analysed field covers the *JWST* GOODS-S JADES field imaged with the 4.4, 2.0, and 0.9 μm bands.

of these studies used high redshifts space-based telescopes, these observations can be considered to be in conflict with the observation of unequal distribution shown in Section 3. Analyses of these experiments, including reproduction of the results, show that these experiments are in fact aligned with the non-random distribution as shown in Section 3. Explanations of these experiments as well as code and data to reproduce them can be found in Shamir (2023), and description of specific experiments can be found in Shamir (2022c, e) and Mcadam & Shamir (2023b).

One of the early experiments (Iye & Sugai 1991) tested the distribution by annotating the galaxies manually. Besides the limitations of possible systematic biases of manual annotations, manual annotation is also highly limited by the volume of data that can be processed. The resulting data set only included 3257 galaxies rotating clockwise and 3268 galaxies rotating counterclockwise. As explained quantitatively in Shamir (2022c, e, 2023), Mcadam & Shamir (2023b), that data set was far too small to show a statistically significant difference for galaxies at relatively low redshift. Experiments using Earth-based telescopes used far larger data sets (Shamir 2022c, e, 2023; Mcadam & Shamir 2023b).

An experiment that received public attention was made by using anonymous volunteers to annotate the galaxies through the Internet

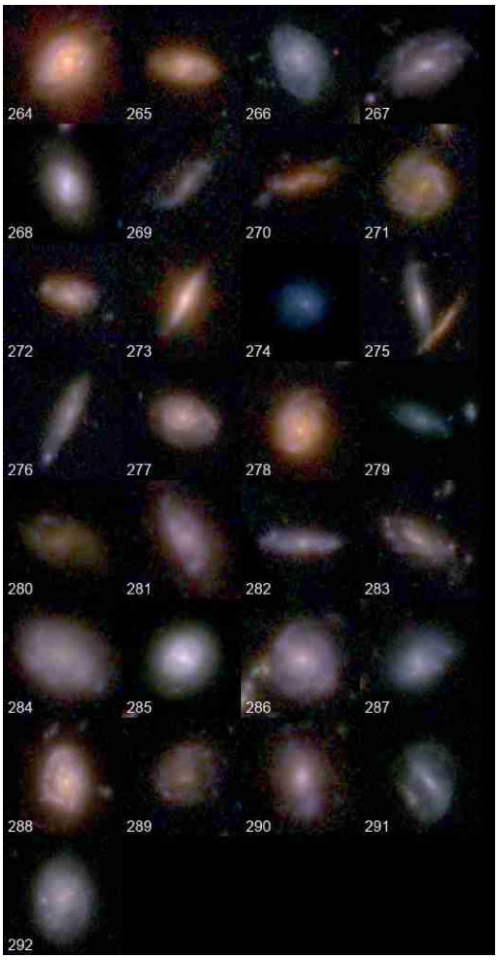

Figure 8. The galaxies in the JADES GOODS-S field that were not identified by the annotation algorithm, but were identified through manual inspection as galaxies that could be rotating in the same direction relative to the Milky Way (counterclockwise). The direction of rotation in these galaxies is not entirely clear from the images.

(Land et al. 2008). The use of a large number of human annotators provided a large number of annotations. The downside of the approach was that the annotations made by the volunteers had a substantial degree errors, making most annotated galaxies unusable due to the high level of disagreements between the annotators. More importantly, the human annotators had a bias towards galaxies that rotate counterclockwise, leading to an extreme bias of ∼15 per cent in the resulting 'superclean' data set. That bias did not allow to determine whether the excessive number of galaxies that rotate counterclockwise is driven by the Universe or by the bias of the volunteers who annotated them.

After the bias was noticed, a new experiment was done by annotating the original galaxy images as well as the mirrored images. But because the bias was noticed only after a very high number of galaxies were already annotated, the data set of the new experiment was relatively small, and included just $\sim 1.1 \times 10^4$ annotated galaxies. The results are displayed in table 2 in Land et al. (2008). As also explained in Shamir (2022c, e, 2023, 2024e) and Mcadam & Shamir (2023b), the table shows a 1.5 per cent higher number of galaxies rotating counterclockwise in the first experiment, and 2.2 per cent in the second experiment. Due to the small number of galaxies the statistical significance was marginal, and becomes significant only

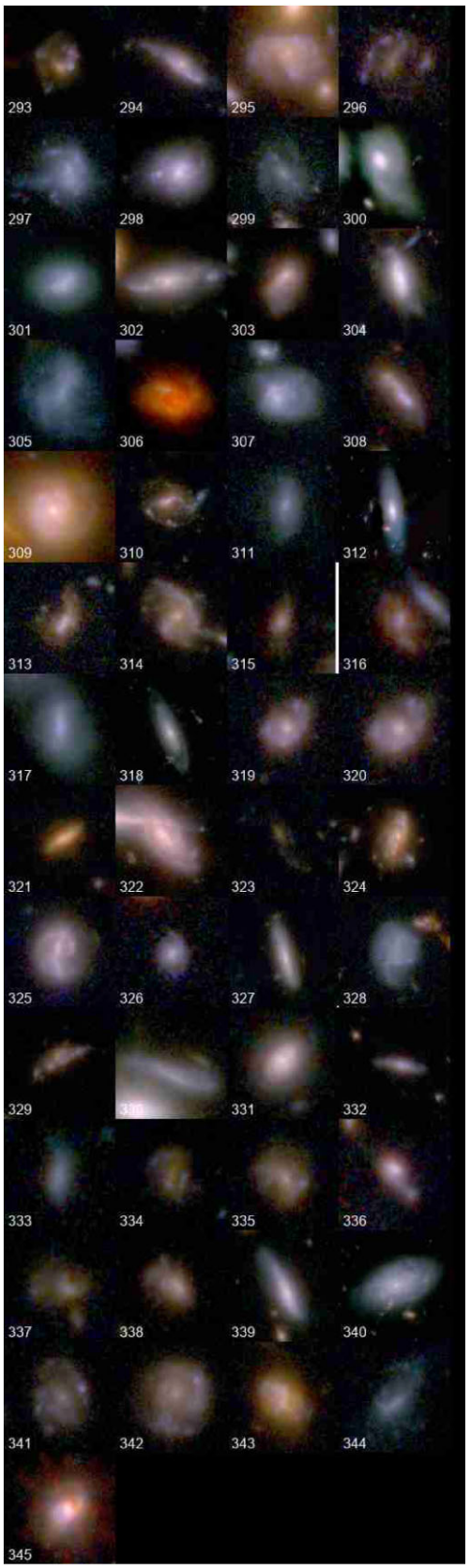

Figure 9. The galaxies in the JADES GOODS-S field that were not identified by the annotation algorithm, but were identified manually as galaxies that could be rotating in the opposite direction relative to the Milky Way.

Table 3. The RA and Dec. of the galaxies that rotate counterclockwise shown in Fig. 8.

Numbers	RA	Dec.	Numbers	RA	Dec.	Numbers	RA	Dec.
264	53.0384867	−27.8622052	265	53.0502416	−27.8402054	266	53.0571043	−27.8209306
267	53.0734400	−27.8408036	268	53.0784400	−27.8194916	269	53.0938238	−27.8941047
270	53.0960714	−27.8286830	271	53.0968709	−27.8855638	272	53.0979105	−27.9080514
273	53.1119073	−27.8053042	274	53.1205041	−27.8517213	275	53.1315577	−27.8963155
276	53.1329688	−27.8984036	277	53.1393988	−27.7674556	278	53.1411431	−27.7618807
279	53.1435404	−27.7557315	280	53.1500039	−27.7577261	281	53.1523614	−27.7780246
282	53.1588635	−27.7574229	283	53.1607380	−27.8358968	284	53.1644578	−27.7659101
285	53.1673684	−27.8405377	286	53.1675621	−27.7925632	287	53.1807708	−27.7568397
288	53.1812865	−27.7656881	289	53.1821604	−27.8058583	290	53.1898988	−27.7413466
291	53.2070911	−27.7641427	292	53.2093471	−27.7609204			

Table 4. The RA and Dec. of the galaxies that rotate clockwise shown in Fig. 9.

Numbers	RA	Dec.	Numbers	RA	Dec.	Numbers	RA	Dec.
293	53.0307616	−27.8706095	294	53.0331686	−27.8480343	295	53.0477066	−27.8353006
296	53.0552493	−27.8233445	297	53.0608612	−27.8204453	298	53.0689281	−27.8263187
299	53.0697976	−27.8391838	300	53.0711214	−27.8227704	301	53.0741950	−27.8239991
302	53.0882270	−27.8506168	303	53.0923399	−27.8479983	304	53.0965038	−27.9073124
305	53.1072662	−27.8058498	306	53.1074781	−27.8041212	307	53.1082963	−27.8930911
308	53.1184803	−27.8053588	309	53.1198685	−27.7987721	310	53.1228467	−27.8483623
311	53.1284391	−27.8504606	312	53.1360779	−27.8292005	313	53.1403351	−27.8635211
314	53.1413943	−27.8257229	315	53.1419006	−27.8253096	316	53.1436493	−27.7582272
317	53.1452409	−27.7511319	318	53.1508174	−27.7601240	319	53.1508706	−27.8612319
320	53.1508807	−27.8611853	321	53.1547878	−27.7739138	322	53.1548761	−27.8578577
323	53.1554620	−27.8386084	324	53.1557427	−27.7794153	325	53.1588282	−27.7705852
326	53.1600134	−27.8637361	327	53.1602644	−27.8255784	328	53.1608377	−27.8653308
329	53.1639085	−27.7653675	330	53.1692446	−27.7917806	331	53.1707031	−27.7512668
332	53.1713223	−27.7930262	333	53.1729254	−27.7387797	334	53.1763369	−27.8251897
335	53.1788946	−27.7547901	336	53.1814716	−27.8318782	337	53.1818135	−27.8306672
338	53.1825614	−27.8244443	339	53.1830999	−27.7510514	340	53.1901582	−27.7652015
341	53.1907319	−27.7570106	342	53.1926134	−27.7581417	343	53.2021859	−27.7550068
344	53.2023063	−27.7904402	345	53.2180747	−27.7616774			

when combining the two experiments (Shamir 2022c, 2023, 2024e; Mcadam & Shamir 2023b). But the asymmetry agrees on both the direction and the magnitude with the asymmetry shown in Shamir (2020d), which uses the same telescope and same footprint as the experiment of Land et al. (2008).

Hayes et al. (2017) used automation to annotate a large number of galaxies from the same telescope and footprint used in Land et al. (2008) and Shamir (2020d). The results are summarized in table 2 in Hayes et al. (2017), showing consistent results of an excessive number of galaxies that rotate counterclockwise. The experiment that provided random distribution was an experiment done by selecting the spiral galaxies by applying machine learning. Interestingly, the selection of the galaxies by using machine learning was done such that features that correlate with the direction of rotation of the galaxies were identified and removed manually. As stated in Hayes et al. (2017), 'We choose our attributes to include some photometric attributes that were disjoint with those that Shamir (2016) found to be correlated with chirality, in addition to several SpArcFiRe outputs with all chirality information removed'. The discussion does not specify a reason for the decision to manually remove just these features.

After removing these features manually, the analysis provided random distribution. But that can also be expected because removing just the features that can identify galaxy direction of rotation would naturally weaken any signal of unequal number of galaxies that rotate in opposite direction. That is explained in detail in Mcadam & Shamir (2023b), as well as in Shamir (2023). Reproduction of the experiment of Hayes et al. (2017) by using the exact same code and same data but without manually removing specific features showed a clear statistically significant asymmetry (Mcadam & Shamir 2023b), in good agreement with the asymmetry observed with SDSS and other telescopes. The full reproduction of the experiment with code and data is described in Mcadam & Shamir (2023b).

Another experiment used image data taken from the Hyper Suprime-Cam (HCS), and annotated it automatically using a deep neural network (Tadaki et al. 2020). That data analysis provided 38 718 galaxies that rotating clockwise and 37 917 galaxies rotating counterclockwise. Using simple binomial distribution, the one-tailed mere chance probability of the difference is $p \simeq 0.0019$. The higher number of galaxies that rotate clockwise agrees with the location of HCS footprint, which is closer to the Southern Galactic pole. As shown in Shamir (2022e) and in Fig. 10, a higher number of galaxies rotating clockwise is expected at around the Southern Galactic pole.

Since the deep neural network used for the annotation had a certain degree of error, and the error was higher than the asymmetry, the analysis was not considered statistically significant. But although the results cannot be considered a sound proof for the unequal distribution, they are in agreement with the other previous reports that show an unequal number of galaxies that rotate in opposite directions, and certainly do not conflict with them.

Jia, Zhu & Pen (2023) used deep neural networks to study the distribution of galaxy directions of rotation using data collected by

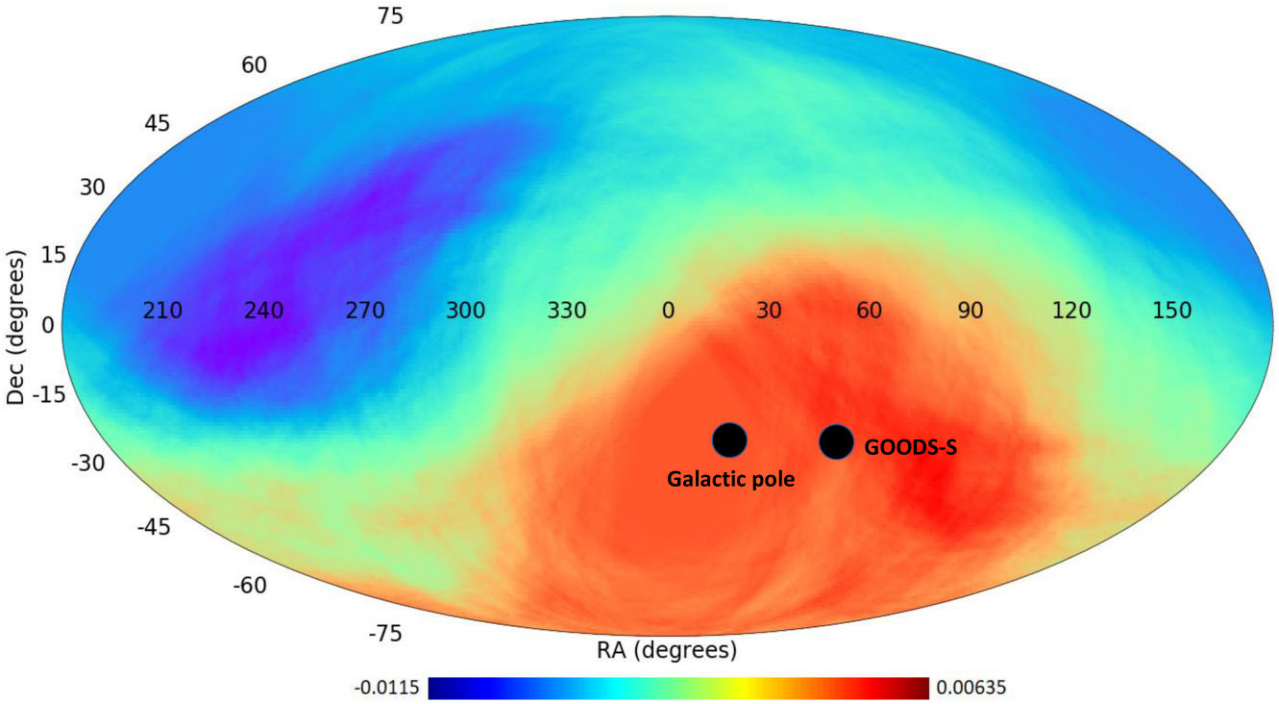

Figure 10. The differences in the number of galaxies with opposite directions of rotations in different parts of the sky as determined by using 1.3×10^6 galaxies imaged by the DESI Legacy Survey (Shamir 2022e). The location of the GOODS-S field is at a part of the sky with a higher number of galaxies rotating clockwise.

SDSS and DESI. Due to the error in the annotation of the neural network, the experiment was done with different accuracy thresholds to balance between the accuracy of the annotations and the size of the data set. When increasing the accuracy threshold, the error in the annotation of the data decreases, but the size of the data set gets smaller since fewer galaxies meet the threshold.

The highest threshold used was 0.9, providing a data set of 9218 SDSS clockwise galaxies and 9442 counterclockwise SDSS galaxies, as shown in table 1 in Jia et al. (2023). The asymmetry of ∼2.4 per cent agrees with the asymmetry shown in Shamir (2020d), which is based on the same sky survey and therefore similar footprint. The one-tailed probability for the observation to occur by mere chance is ∼0.05. That statistical significance is somewhat weaker than the statistical significance observed in Shamir (2020d), which can be expected due to the much higher number of galaxies used in Shamir (2020d). But although the p value is lower, it can still be considered statistically significant, and definitely not in conflict with the other observations as explained in Shamir (2024e).

The DESI Legacy Survey has a very large footprint that covers both hemispheres, and therefore it is difficult to predict the asymmetry as the asymmetry in one hemisphere is offset by the inverse asymmetry in the opposite hemispheres (Shamir 2024e). The analysis of Jia et al. (2023) found 11 649 clockwise galaxies and 11 919 counterclockwise galaxies. The probability of that asymmetry to occur by chance is 0.04. While the large footprint does not allow accurate analysis, the binomial distribution can be considered statistically significant, and does not conflict with the contention that the distribution of the directions of rotation of the galaxies is random.

Another experiment suggesting random distribution of galaxy directions of rotation claimed that the asymmetry shown in previous experiments is the result of 'duplicate objects' in the data set (Iye et al. 2021). This experiment is explained in detail and full reproduction in Shamir (2022c, e, 2023). In summary, the catalogue used in Iye et al. (2021) was used in Shamir (2017b) for photometric analysis only, and no claim for a dipole axis formed by the distribution of the directions of rotation of galaxies was made based on that data set (Shamir 2022c, e, 2023).

More importantly, as shown in Shamir (2023), the reproduction of the experiment using the same data and same analysis method used in Iye et al. (2021) provides different results than the results shown in Iye et al. (2021), showing a statistically significant non-random distribution (Shamir 2023). Code and data that allows to easily reproduce the experiment are available at.[1] The link also provides the description of the reproduction of the National Astronomical Observatory of Japan (NAOJ) to explain the difference between the reproduction and the results shown in the paper. In summary, the NAOJ explains that 'Because it is hard to verify the detail of simulations, we here calculate the analytic solution by Chandrasekhar (1943) which assumes uniform samples in the hemisphere'. But the assumption of a uniform sample is not correct for SDSS, which covers just a part of the hemisphere, and the density of the galaxy population varies substantially within its footprint. That assumption is not mentioned in Iye et al. (2021), and in fact is not needed since the exact locations of all galaxies are well known.

Another study (Patel & Desmond 2024) that suggested the distribution of the directions of rotation of galaxies is random was based on data used in previous studies (Longo 2011; Mcadam & Shamir 2023b). Instead of using the standard binomial distribution statistics and simple χ^2 statistics used in MacGillivray & Dodd (1985), Longo (2011), Shamir (2012, 2016, 2019, 2020b, c, d, 2021a, b, 2022a, b, d, e, 2023, 2024e), and Mcadam & Shamir

[1] https://people.cs.ksu.edu/~lshamir/data/iye_et_al

(2023b), Patel & Desmond (2024) propose a new complex ad-hoc statistical method. The downside of the new method is that it does not respond to asymmetry in the distribution of galaxy spin directions (Shamir 2024a, d). As explained in Shamir (2024a), even in cases where synthetic asymmetry is added to the data to create a highly asymmetric data set, the method still reports random distribution.

For instance, Patel & Desmond (2024) applied the new method to the data set used in Mcadam & Shamir (2023b), annotated as 'GAN M' in Patel & Desmond (2024). It is publicly available at https://people.cs.ksu.edu/~lshamir/data/sparcfire/. The data set was annotated by the *SpArcFiRe* algorithm for the purpose of reproducing the results shown in Hayes et al. (2017), not necessarily to study the Universe due to the known bias in the annotation method. As noted in the appendix of Hayes et al. (2017), *SpArcFiRe* has a known bias, and therefore a dataset annotated by it is expected to show a difference between the number of galaxies rotating clockwise and the number of galaxies rotating counterclockwise. Indeed, the data set of 139 852 galaxies annotated by *SpArcFiRe* is separated to 70 672 counterclockwise galaxies and 69 180 clockwise galaxies. Using standard binomial statistics, the two-tailed probability to have such asymmetry by chance is ~ 0.00006. But as reported in the fourth row of table 4 in Patel & Desmond (2024), the new statistical method provided a non-significant p-value of 0.25. The fact that applying the new method to an extremely asymmetric synthetic data shows a null-hypothesis universe with no statistically significant asymmetry, indicating that the new method does not guarantee to identify asymmetry (Patel & Desmond 2024).

Patel & Desmond (2024) also argued that the reproduction of previous results of Longo (2011) and Mcadam & Shamir (2023b) provided different results than the results stated in these papers, as stated in section 4.3 in Patel & Desmond (2024). That claim has also shown to be incorrect, with code and step-by-step instructions to easily reproduce the results of both papers. The full open code and step-by-step instructions can be found at https://people.cs.ksu.edu/~lshamir/data/patel_desmond/.

5 CONCLUSION

JWST has provided unprecedented imaging power that allows to observe high visual details of galaxies in the deep Universe. Despite being relatively new, observations made in *JWST* deep fields have already challenged some of the foundational assumptions regarding the Universe. Here, *JWST* shows that the number of galaxies that rotate in the opposite direction relative to the Milky Way as observed from Earth is higher than the number of galaxies that rotate in the same direction relative to the Milky Way. The observation was made also with initial *JWST* data (Shamir 2024e), and was also noticed in the UDF imaged by *HST* (Shamir 2021c), but JADES allows to observe the asymmetry in the early Universe using a much higher number of galaxies. The analysis is done by a defined quantitative criteria, but the asymmetry is high and can be inspected also by the unaided human eye.

As discussed in Introduction, the asymmetry between galaxies that rotate in opposite directions was noticed in numerous studies starting the 1980s, and more recent experiments include analysis of very large data sets collected by autonomous digital sky surveys. The magnitude of the asymmetry observed through *JWST* is stronger than the magnitude of the asymmetry reported previously using Earth-based data. That can be linked to the previous observation that the magnitude of the asymmetry increases as the redshift gets higher (Shamir 2019, 2020d, 2022d, 2024d). For instance, table 5, taken from Shamir (2020d), shows the distribution of spiral galaxies imaged by SDSS at different redshift ranges. The RA is limited to (120°, 210°), which is around the location of the Northern end of the Galactic pole.

Table 5. The distribution of galaxies rotating clockwise and counterclockwise imaged by SDSS. All galaxies are within the RA range of (120°, 210°). The p-values are the binomial distribution p-value to have such asymmetry or stronger by chance. The table is taken from Shamir (2020d).

z	cw	ccw	$\frac{\text{cw}}{\text{cw+ccw}}$	p-value
0–0.05	3216	3180	0.5003	0.698
0.05–0.1	6240	6270	0.498	0.4
0.1–0.15	4236	4273	0.496	0.285
0.15–0.2	1586	1716	0.479	0.008
0.2–0.5	2598	2952	0.469	1.07×10^{-6}
Total	17 876	18 391	0.493	0.0034

As the table shows, the asymmetry increases as the redshift gets higher. While there is no proven link between the observation made with *JWST* and the information provided in Table 5, it should remain a possibility that the observations are linked. In that case, the asymmetry changes gradually with time or distance from Earth.

Possible explanations to the observation can be broadly divided into two categories: the first is an anomaly in the large-scale structure (LSS) of the early universe, and the second is related to the physics of galaxy rotation.

5.1 Anomaly in the LSS

If the observation shown here indeed reflects the structure of the Universe, it shows that the early universe was more homogeneous in terms of the directions towards which galaxies rotate, and becomes more chaotic over time while exhibiting a cosmological-scale axis that is close to the Galactic pole. Some cosmological models assume a geometry that features a cosmological-scale axis. These include ellipsoidal Universe (Campanelli, Cea & Tedesco 2006, 2007; Gruppuso 2007; Campanelli et al. 2011; Cea 2014), dipole big bang (Allahyari et al. 2025; Krishnan, Mondol & Sheikh-Jabbari 2023), and isotropic inflation (Feng & Zhang 2003; Piao, Feng & Zhang 2004; Bohmer & Mota 2008; Edelstein, Rodríguez & López 2020; Arciniega et al. 2020a; Arciniega, Edelstein & Jaime 2020b; Jaime 2021; Dainotti et al. 2022; Luongo et al. 2022). In these cases, the large-scale distribution of the galaxy rotation is aligned in the form of a cosmological-scale axis, and the location of that axis in close proximity to the Galactic pole can be considered a coincidence.

An additional cosmological model that requires the assumption of a cosmological-scale axis is the theory of rotating Universe (Gödel 1949; Ozsváth & Schücking 1962; Ozsvath & Schücking 2001; Sivaram & Arun 2012; Chechin 2016; Campanelli 2021; Seshavatharam & Lakshminarayana 2021). That model is also related to the theory of black hole cosmology (Pathria 1972; Stuckey 1994; Easson & Brandenberger 2001; Tatum et al. 2018; Chakrabarty et al. 2020), according which the Universe is the interior of black hole in a parent universe, and therefore is also aligned with the contention of multiverse.

Because black holes spin (McClintock et al. 2006; Mudambi et al. 2020; Reynolds 2021), a universe hosted inside of a black hole is also expected to spin. Therefore, it has been proposed that a universe located in the interior of a black hole should have an axis, and inherit the preferred direction of the host black hole (Popławski 2010; Seshavatharam 2010; Christillin 2014; Seshavatharam &

Lakshminarayana 2020, 2021). Black hole cosmology is also linked to the theory of holographic universe (Susskind 1995; Bak & Rey 2000; Bousso 2002; Myung 2005; Hu & Ling 2006; Sivaram & Arun 2013; Shor, Benninger & Khrennikov 2021; Rinaldi et al. 2022).

Another paradigm relevant to the observation described here is the contention that the LSS of the Universe has a fractal structure, reflected by fractal patterns formed by the large-scale distribution galaxies (Baryshev et al. 1998; Baryshev 2000; Pietronero & Labini 2000; Labini & Pietronero 2001; Labini & Gabrielli 2003, 2004; Gabrielli et al. 2005; Teles, Lopes & Ribeiro 2022). These patterns challenge the assumption that the distribution of galaxies in the LSS is random.

These explanations are considered alternative to the standard cosmological model (Turner 1996; Pecker 1997; Perivolaropoulos 2014; Bull et al. 2016; Netchitailo et al. 2020; Velten & Gomes 2020), and also violates the isotropy assumption of the Cosmological Principle. Although the Cosmological Principle is the basic assumption for the standard cosmological model, its correctness has been challenged (Pecker 1997; Kroupa 2012). Observations using a variety of different probes have also challenged the correctness of the Cosmological Principle in an empirical manner (Aluri et al. 2023).

5.2 Physics of galaxy rotation

As mentioned above, if the distribution of directions of rotation of galaxies indeed form a cosmological-scale axis, the alignment of that axis with the Galactic pole could be considered a coincidence. But another explanation could be that the distribution of galaxy direction of rotation in the Universe is random, but only seems non-random to an Earth-based observer. In that case, the observation can be explained by the effect of the rotational velocity of the observed galaxies relative to the rotational velocity of Earth around the centre of the Milky Way galaxy. That can explain the observation without violating the Cosmological Principle. The proximity to the Galactic pole is expected, as the difference between the rotational velocity of the Milky Way and the rotational velocity of the observed galaxies peaks at the Galactic pole.

As discussed in Shamir (2017a, 2020a) and McAdam & Shamir (2023a), due to the Doppler shift effect galaxies that rotate in the opposite direction relative to the Milky Way are expected to be slightly brighter than galaxies that rotate in the same direction relative to the Milky Way. Therefore, more galaxies that rotate in the opposite direction relative to the Milky Way are expected to be observed from Earth, and the difference should peak at around the Galactic pole. That observation is conceptually aligned with the empirical data of Fig. 10, and the observation using JADES described in Section 3.

This explanation is challenged by the fact that the effect of the rotational velocity have merely a mild impact on the brightness of galaxies, and therefore is not expected to lead to the dramatic difference of ∼50 per cent in the number of galaxies as observed through JADES. On the other hand, empirical observations showed that the difference in brightness is larger than expected given the rotational velocity of galaxies (Shamir 2017a, 2020a; McAdam & Shamir 2023a). That was observed with SDSS (McAdam & Shamir 2023a), Pan-STARRS (Shamir 2017a), and the space-based *HST* (Shamir 2020a). Similar observations were made with the redshift (Shamir 2024b, c), also showing that the magnitude of the asymmetry increases as the redshift gets larger (Shamir 2024b). Other related observations can be the dipole formed by quasar distribution as observed from Earth (Hutsemékers et al. 2014; Secrest et al. 2021), which has been shown to be linked to the colour (Panwar, Jain & Omar 2024), and therefore could also be a photometric effect rather than a feature of the LSS of the Universe. The number of galaxies in the line of sight also show a surprising cosmological-scale anisotropy (Ahn 2025), and that can also be related to the differences in the brightness of galaxies as observed from Earth.

The difference can be linked to the mysterious physics of galaxy rotation, which is known to be in substantial tension with the mass (Oort 1940; Rubin 1983). Common explanations include dark matter (Rubin 1983; El-Neaj et al. 2020), modified Newtonian dynamics (Milgrom 1983), and others (Sanders 1990; Capozziello & De Laurentis 2012; Chadwick, Hodgkinson & McDonald 2013; Farnes 2018; Nagao 2020; Rivera 2020; Blake 2021; Gomel & Zimmerman 2021; Skordis & Złośnik 2021; Larin 2022), but no explanation has been fully proven. In particular, the theory of dark matter as the explanation to the difference between the mass and rotational velocity of stars within galaxies has been challenged, and despite over a century of research there is still no clear proven explanation to the physics of galaxy rotation (Sanders 1990; Mannheim 2006; Kroupa 2012, 2015; Kroupa, Pawlowski & Milgrom 2012; Akerib et al. 2017; Arun, Gudennavar & Sivaram 2017; Aprile et al. 2018; Bertone & Tait 2018; Skordis & Złośnik 2019; Hofmeister & Criss 2020; Sivaram, Arun & Rebecca 2020; Byrd & Howard 2021). Therefore, it is possible that the physics of galaxy rotation, which is not yet fully known, affects the brightness of the galaxy in a manner that is not necessarily expected.

If the physics of galaxy rotation affects the light that galaxies emit in a manner that is currently unknown, that can also affect the redshift, and therefore can be related to alternative redshift models (Crawford 1999; Shao 2013; Kragh 2017; Shao, Wang & Gao 2018; Sato 2019; LaViolette 2021; Lovyagin et al. 2022; Fulton 2023; Lee 2023; Lopez-Corredoira 2023; Pletcher 2023; Seshavatharam & Lakshminarayana 2023; Gupta 2024a). Although the physical mechanism of such phenomenon is not clear, using alternative redshift models can explain a large number of observations that are currently unexplained such as dark energy, the H_o tension (Wu & Huterer 2017; Bolejko 2018; Mörtsell & Dhawan 2018; Davis et al. 2019; Camarena & Marra 2020; Pandey et al. 2020; Di Valentino et al. 2021; Riess et al. 2022), as well as the unexpected presence of large and massive galaxies in the early Universe (Xiao et al. 2024; Glazebrook et al. 2024) that challenge the age of the Universe as estimated by the existing models. The age of the Universe has been challenged also by the presence of stars that are older than the estimated age of the Universe such as HD 140283 (Guillaume et al. 2024). These tensions challenge modern cosmology, and trigger a variety of solutions and explanations that involve new physics. These puzzling observations can be solved by using an alternative the redshift model (Crawford 1999; Shao 2013, 2019; Kragh 2017; Shao et al. 2018; LaViolette 2021; Lovyagin et al. 2022; Fulton 2023; Gupta 2023, 2024a; Lee 2023; Lopez-Corredoira 2023; Pletcher 2023; Seshavatharam & Lakshminarayana 2023). Although the physics that can lead to alternative redshift models is also not yet known, it can explain the observed tensions regarding the expansion rate and age of the Universe.

The unprecedented power of *JWST*, combined with other recent observations have revolutionized cosmology, and triggered substantial changes in the studying of the Universe. It is likely that research efforts to explain them will continue in the next few decades. The observation reported here can provide yet another piece of information that can ultimately lead to a complete model that can provide a consolidated explanation to all current unexplained observations.

ACKNOWLEDGEMENTS

I would like to thank the knowledgeable reviewer and associate editor for the insightful comments. The study was supported in part by National Science Foundation grant 2148878.

DATA AVAILABILITY

The data used in this study are available in the tables included in the manuscript. URLs to relevant data sets from previous papers are also provided in the body of the manuscript.

REFERENCES

Adams N. et al., 2023, MNRAS, 518, 4755
Adil S. A., Mukhopadhyay U., Sen A. A., Vagnozzi S., 2023, J. Cosmol. Astropart. Phys., 2023, 072
Ahn K., 2025, J. Korean Phys. Soc., 86, 145
Akerib D. S. et al., 2017, Phys. Rev. Lett., 118, 021303
Allahyari A., Ebrahimian E., Mondol R., Sheikh-Jabbari M., 2025, Eur. Phys. J. C., 85, 119
Aluri P. K. et al., 2023, Class. Quantum Gravity, 40, 094001
Aprile E. et al., 2018, Phys. Rev. Lett., 121, 111302
Arciniega G., Bueno P., Cano P. A., Edelstein J. D., Hennigar R. A., Jaime L. G., 2020a, Phys. Lett. B, 802, 135242
Arciniega G., Edelstein J. D., Jaime L. G., 2020b, Phys. Lett. B, 802, 135272
Arun K., Gudennavar S., Sivaram C., 2017, Adv. Space Res., 60, 166
Bak D., Rey S.-J., 2000, Class. Quantum Gravity, 17, L1
Ball P., 2023, Nature, 624, 22
Baryshev Y. V., 2000, Astron. Astrophys. Trans., 19, 417
Baryshev Y. V., Labini F. S., Montuori M., Pietronero L., Teerikorpi P., 1998, Fractals, 06, 231
Bertone G., Tait T. M., 2018, Nature, 562, 51
Blake B. C., 2021, Bull. Am. Phys. Soc., 2021, B17.00002
Bohmer C. G., Mota D. F., 2008, Phys. Lett. B, 663, 168
Bolejko K., 2018, Phys. Rev. D, 97, 103529
Bousso R., 2002, Rev. Mod. Phys., 74, 825
Boylan-Kolchin M., 2023, Nat. Astron., 7, 731
Bradley L. D. et al., 2023, ApJ, 955, 13
Bull P. et al., 2016, Phys. Dark Universe, 12, 56
Bunker A. J. et al., 2024, A&A, 690, A288
Byrd G., Howard S., 2019, J. Wash. Acad. Sci., 105, 1
Byrd G., Howard S., 2021, J. Wash. Acad. Sci., 107, 1
Camarena D., Marra V., 2020, Phys. Rev. Res., 2, 013028
Campanelli L., 2021, Found. Phys., 51, 56
Campanelli L., Cea P., Fogli G., Tedesco L., 2011, Mod. Phys. Lett. A, 26, 1169
Campanelli L., Cea P., Tedesco L., 2006, Pjys. Rev. Lett., 97, 131302
Campanelli L., Cea P., Tedesco L., 2007, Phys. Rev. D, 76, 063007
Capozziello S., De Laurentis M., 2012, Ann. Phys., 524, 545
Carniani S. et al., 2024, Nature, 633, 318
Cea P., 2014, MNRAS, 441, 1646
Chadwick E. A., Hodgkinson T. F., McDonald G. S., 2013, Phys. Rev. D, 88, 024036
Chakrabarty H., Abdujabbarov A., Malafarina D., Bambi C., 2020, Eur. Phys. J. C, 80, 1
Chechin L., 2016, Astron. Rep., 60, 535
Christillin P., 2014, Eur. Phys. J. Plus, 129, 1
Costantin L. et al., 2023, Nature, 623, 499
Crawford D. F., 1999, Aust. J. Phys., 52, 753
Dainotti M. G., De Simone B., Schiavone T., Montani G., Rinaldi E., Lambiase G., Bogdan M., Ugale S., 2022, Galaxies, 10, 24
Davis T. M., Hinton S. R., Howlett C., Calcino J., 2019, MNRAS, 490, 2948
De Vaucouleurs G., 1958, ApJ, 127, 487
Dhar S., Shamir L., 2021, Visual Inform., 5, 92
Dhar S., Shamir L., 2022, A&C, 38, 100545
Di Valentino E. et al., 2021, Class. Quantum Gravity, 38, 153001
Dolgov A., 2023, preprint (arXiv:2310.00671)
Easson D. A., Brandenberger R. H., 2001, J. High Energy Phys., 2001, 024
Edelstein J. D., Rodríguez D. V., López A. V., 2020, J. Cosmol. Astropart. Phys., 2020, 040
Eisenstein D. J. et al., 2023, preprint (arXiv:2306.02465)
El-Neaj Y. A. et al., 2020, EPJ Quant. Technol., 7, 1
Erukude S. T., Joshi A., Shamir L., 2024, Computers, 13, 341
Farnes J. S., 2018, A&A, 620, A92
Feng B., Zhang X., 2003, Phys. Lett. B, 570, 145
Forconi M., Melchiorri A., Mena O., Menci N., et al., 2023, J. Cosmol. Astropart. Phys., 2023, 012
Freeman T., Byrd G., Howard S., 1991, BASS, 23, 1460
Fulton D., 2023, Cosmological Redshift via Non-Linear Frequency Down-Conversion of Electromagnetic Radiation.
Gabrielli A., Labini F. S., Joyce M., Pietronero L., 2005, Statistical Physics for Cosmic Structures. Springer-Verlag, Berlin, p. 101
Glazebrook K. et al., 2024, Nature, 628, 277
Gödel K., 1949, Rev. Mod. Phys., 21, 447
Gomel R., Zimmerman T., 2021, Galaxies, 9, 34
Gruppuso A., 2007, Phys. Rev. D, 76, 083010
Guillaume C., Buldgen G., Amarsi A., Dupret M., Lundkvist M., Larsen J., Scuflaire R., Noels A., 2024, A&A, 692, L3
Gupta R. P., 2023, MNRAS, 524, 3385
Gupta R. P., 2024b, Universe, 10, 266
Gupta R., 2024a, ApJ, 964, 55
Hayes W. B., Davis D., Silva P., 2017, MNRAS, 466, 3928
Helton J. M. et al., 2024, preprint (arXiv:2405.18462)
Hofmeister A. M., Criss R. E., 2020, Galaxies, 8, 54
Hu B., Ling Y., 2006, Phys. Rev. D, 73, 123510
Hutsemékers D., Braibant L., Pelgrims V., Sluse D., 2014, A&A, 572, A18
Iye M., Sugai H., 1991, ApJ, 374, 112
Iye M., Tadaki K., Fukumoto H., 2019, ApJ, 886, 133
Iye M., Yagi M., Fukumoto H., 2021, ApJ, 907, 123
Jaime L. G., 2021, Phys. Dark Universe, 34, 100887
Jain R., Wadadekar Y., 2024, preprint (arXiv:2412.04834)
Jia H., Zhu H.-M., Pen U.-L., 2023, ApJ, 943, 32
Jones G. C. et al., 2025, MNRAS, 536, 2355
Kragh H., 2017, J. Astron. Hist. Her., 20, 2
Krishnan C., Mondol R., Sheikh-Jabbari M., 2023, J. Cosmol. Astropart. Phys., 2023, 020
Kroupa P., 2012, Publ. Astron. Soc. Aust., 29, 395
Kroupa P., 2015, Can. J. Phys., 93, 169
Kroupa P., Pawlowski M., Milgrom M., 2012, Int. J. Mod. Phys. D, 21, 1230003
Kuhn V., Guo Y., Martin A., Bayless J., Gates E., Puleo A., 2024, ApJ, 968, L15
Labini F. S., Gabrielli A., 2003, Institute of Physics Conference Series. Institute of Physics, Philadelphia, p. 305
Labini F. S., Gabrielli A., 2004, Phys. A: Stat. Mech. Appl., 338, 44
Labini F. S., Pietronero L., 2001, Phase Transitions in the Early Universe: Theory and Observations. Springer, Dordrecht
Land K. et al., 2008, MNRAS, 388, 1686
Larin S. A., 2022, Universe, 8, 632
LaViolette P. A., 2021, Int. J. Astron. Astrophys., 11, 190
Lee S., 2023, Phys. Dark Universe, 42, 101286
Longo M. J., 2011, Phys. Lett. B, 699, 224
Lopez-Corredoira M., 2023, preprint (arXiv:2307.10606)
Lovell C. C., Harrison I., Harikane Y., Tacchella S., Wilkins S. M., 2023, MNRAS, 518, 2511
Lovyagin N., Raikov A., Yershov V., Lovyagin Y., 2022, Galaxies, 10, 108
Luongo O., Muccino M., Colgáin E. Ó., Sheikh-Jabbari M., Yin L., 2022, Phys. Rev. D, 105, 103510
MacGillivray H., Dodd R., 1985, A&A, 145, 269
Mannheim P. D., 2006, Prog. Part. Nucl. Phys., 56, 340
McAdam D., Shamir L., 2023a, Symmetry, 15, 1190
Mcadam D., Shamir L., 2023b, Adv. Astron., 2023, 1
McClintock J. E., Shafee R., Narayan R., Remillard R. A., Davis S. W., Li L.-X., 2006, ApJ, 652, 518

Melia F., 2023, MNRAS, 521, L85
Milgrom M., 1983, AJ, 270, 365
Morháč M., Kliman J., Matoušek V., Veselskỳ M., Turzo I., 2000, Nucl. Instrum. Methods Phys. Res. A, 443, 108
Mörtsell E., Dhawan S., 2018, J. Cosmol. Astropart. Phys., 2018, 025
Mudambi S. P., Rao A., Gudennavar S., Misra R., Bubbly S., 2020, MNRAS, 498, 4404
Muñoz J. B., Mirocha J., Chisholm J., Furlanetto S. R., Mason C., 2024, MNRAS, 535, L37
Myung Y. S., 2005, Phys. Lett. B, 610, 18
Nagao S., 2020, Rep. Adv. Phys. Sci., 04, 2050004
Netchitailo V. S. et al., 2020, J. High Energy Phys. Gravit. Cosmol., 06, 133
Oort J. H., 1940, AJ, 91, 273
Ozsváth I., Schücking E., 1962, Nature, 193, 1168
Ozsvath I., Schücking E., 2001, Class. Quantum Gravity, 18, 2243
Pandey S., Raveri M., Jain B., 2020, Phys. Rev. D, 102, 023505
Panwar M., Jain P., Omar A., 2024, MNRAS, 535, L63
Patel D., Desmond H., 2024, MNRAS, 534, 1553
Pathria R., 1972, Nature, 240, 298
Pecker J.-C., 1997, JA&A, 18, 323
Perivolaropoulos L., 2014, Galaxies, 2, 22
Piao Y.-S., Feng B., Zhang X., 2004, Phys. Rev. D, 69, 103520
Pietronero L., Labini F. S., 2000, Phys. A: Stat. Mech. Appl., 280, 125
Pletcher A. E., 2023, Qeios, 10.32388/2X1GDL.2
Popławski N. J., 2010, Phys. Lett. B, 694, 181
Reynolds C. S., 2021, ARA&A, 59, 117
Riess A. G. et al., 2022, ApJ, 934, L7
Rinaldi E., Han X., Hassan M., Feng Y., Nori F., McGuigan M., Hanada M., 2022, Phys. Rev. X Quant., 3, 010324
Rivera P. C., 2020, Am. J. Astron. Astrophys., 7, 73
Rubin V. C., 1983, Science, 220, 1339
Sanders R., 1990, A&AR, 2, 1
Sato M., 2019, Phys. Essays, 32, 43
Schouws S. et al., 2024, preprint (arXiv:2409.20549)
Secrest N., Hausegger S., Rameez M., Mohayaee R., Sarkar S., Colin J., 2021, ApJ, 908, L51
Seshavatharam U. S., Lakshminarayana S., 2023, Phys. Sci. Forum., 7, 43
Seshavatharam U., 2010, Prog. Phys., 2, 7
Seshavatharam U., Lakshminarayana S., 2020, Int. Astron. Astrophys. Res. J., 10, 247
Seshavatharam U., Lakshminarayana S., 2021, Int. Astron. Astrophys. Res. J., 2, 282
Shamir L., 2011a, Astrophysics Source Code Library, record ascl:1105.011
Shamir L., 2011b, ApJ, 736, 141
Shamir L., 2012, Phys. Lett. B, 715, 25
Shamir L., 2013, Galaxies, 1, 210
Shamir L., 2016, ApJ, 823, 32
Shamir L., 2017a, Publ. Astron. Soc. Aust., 34, e44
Shamir L., 2017b, Publ. Astron. Soc. Aust., 34, e011
Shamir L., 2017c, Ap&SS, 362, 33
Shamir L., 2019, Large-scale patterns of galaxy spin rotation show cosmological-scale parity violation and multipoles, preprint (arXiv:1912.05429)
Shamir L., 2020a, Open Astron., 29, 15
Shamir L., 2020b, Publ. Astron. Soc. Aust., 37, e053
Shamir L., 2020c, Astron. Nachr., 341, 324
Shamir L., 2020d, Ap&SS, 365, 136
Shamir L., 2021a, Particles, 4, 11
Shamir L., 2021b, Publ. Astron. Soc. Aust., 38, e037
Shamir L., 2021c, AAS Meeting, 230, 8
Shamir L., 2022a, Universe, 8, 397
Shamir L., 2022b, JA&A, 43, 24
Shamir L., 2022c, PASJ, 74, 1114
Shamir L., 2022d, Astron. Nachr., 343, e20220010
Shamir L., 2022e, MNRAS, 516, 2281
Shamir L., 2023, Symmetry, 15, 9
Shamir L., 2024a, preprint (arXiv:2404.13864)
Shamir L., 2024b, Particles, 7, 703
Shamir L., 2024c, Universe, 10, 129
Shamir L., 2024d, Symmetry, 16, 1389
Shamir L., 2024e, Publ. Astron. Soc. Aust., 41, e038
Shao M.-H., 2013, Phys. Essays, 26, 183
Shao M.-H., Wang N., Gao Z.-F., 2018, Redefining Standard Model Cosmology. IntechOpen, London, p. 13
Shen X., Vogelsberger M., Boylan-Kolchin M., Tacchella S., Naidu R. P., 2024, MNRAS, 533, 3923
Shor O., Benninger F., Khrennikov A., 2021, Entropy, 23, 584
Sivaram C., Arun K., 2012, Open Astron., 5, 7
Sivaram C., Arun K., 2013, Ap&SS, 348, 217
Sivaram C., Arun K., Rebecca L., 2020, JA&A, 41, 1
Skordis C., Złośnik T., 2019, Phys. Rev. D, 100, 104013
Skordis C., Złośnik T., 2021, Phys. Rev. Lett., 127, 161302
Stuckey W., 1994, Am. J. Phys., 62, 788
Susskind L., 1995, J. Math. Phys., 36, 6377
Tadaki K.-i., Iye M., Fukumoto H., Hayashi M., Rusu C. E., Shimakawa R., Tosaki T., 2020, MNRAS, 496, 4276
Tatum E. T., et al., 2018, J. Mod. Phys., 09, 1867
Teles S., Lopes A. R., Ribeiro M. B., 2022, Eur. Phys. J. C, 82, 896
Tsukui T., Iguchi S., 2021, Science, 372, 1201
Turner M. S., 1996, Phys. World, 9, 31
Velten H., Gomes S., 2020, Phys. Rev. D, 101, 043502
Wang D., Liu Y., 2023, preprint (arXiv:2301.00347)
Wu H.-Y., Huterer D., 2017, MNRAS, 471, 4946
Xiao M. et al., 2024, Nature, 635, 311

This paper has been typeset from a TEX/LATEX file prepared by the author.